Experimental Studies on a Low-Power Duoplasmatron-Type MPD Thruster

Itsuro Kimura* and Ryuhei Kumazawa†
University of Tokyo, Tokyo, Japan

A low-power magnetoplasmadynamic (MPD) thruster, composed of a Duoplasmatron-type plasma source and a magnetic nozzle, has been under study, and experimental results with H_2 propellant already have been reported. This paper describes further systematic experimental investigation made to demonstrate the feasibility of a thruster of this type. It is shown that with more suitable propellants (e.g., Ar, NH_3) the thruster can be operated in relatively high thrust efficiency in the range of moderate specific impulses. It also is shown, using the data obtained by diagnostics of the exhaust plume, that the ionization efficiency of propellent is fairly high, and that the following two electromagnetic acceleration mechanisms exist in this thruster: 1) plasma expansion in the magnetic nozzle; and 2) transformation of rotational energy of ions into kinetic energy of axial direction.

Introduction

MANY studies have been made of low-thrust thrusters for such missions as satellite station-keeping or attitude control. Recently some promising experimental results were reported for low-thrust plasma thrusters (steady or pulsed), which are physically and electrically simpler than electrostatic thrusters and potentially very reliable in operation.[1-3]

Since 1970, a low-power magnetoplasmadynamic (MPD) thruster of the Duoplasmatron type has been under study. The results of experiments with H_2 propellant showed moderate thrust efficiencies in the range of relatively high specific impulse.[4] This paper describes further improvement on the thruster performance achieved by systematic experimental investigation, and also the interior physical process (i.e., the acceleration mechanisms) elucidated by diagnostics of the exhaust plume.

Apparatus and Experimental Procedure

Thruster

Figure 1 shows the Duoplasmatron-type MPD thruster used in this study. It is composed of a Duoplasmatron (an arc-type plasma source due to von Ardenne[5]) and a magnetic nozzle. This plasma source, with its baffle (Zwischenelektrod) and main magnetic coil, can be operated at high ionization efficiency (low neutral emission), with a variety of propellants, by using mechanical or thermal constriction and magnetic constraint.

The operating characteristics of this thruster depend strongly upon the geometry of the electrodes and the magnetic nozzle applied. The details of the electrode geometry used in the experiments for Ar, N_2, and NH_3 propellants (electrode-geometry A) are shown in Fig. 2. In electrode-geometry A, $D_a = 7.0$ mm, $D_b = 4.0$ mm, and $L_{ab} = 4.0$ mm. In electrode-geometry B, used for He and H_2 propellants, $D_a = 3.5$ mm, $D_b = 2.0$ mm, and $L_{ab} = 5.0$ mm.

It must be noticed that, to obtain high performance, D_a must be made larger than D_b. (In this device, the discharge voltage increased generally with increasing arc current, and, for a constant arc current, the discharge voltage increased when D_a is increased or L_{ab} is decreased.) In the present device, the magnetic nozzle is produced by the magnetic coil of the Duoplasmatron itself (main magnetic coil) and that attached to the outside of the anode holder (secondary magnetic coil). The magnetic field in the neighborhood of the anode nozzle is formed mainly by the former, and the latter contributes to shaping the downstream part of the magnetic nozzle. In Fig. 2, the magnetic field map for electrode-geometry A, main magnetic coil current $(I_c) = 6$ A and secondary magnetic coil current $(I_c') = 0$ A, also is shown (obtained by using iron filings). The average density of magnetic flux at the throat of the magnetic nozzle is about 0.36 T in this case.

Thrust Measurement

The experiments were conducted in a 25-cm-diam × 40 cm-long bell jar, and the background pressure was maintained at the level of 10^{-4} Torr throughout the experiments. The thrust was evaluated using a pendulum-type thrust target,[6] measuring its deflection by a differential transformer. A cone shape, facing its base to the thruster, was chosen for the target, which would reduce any error caused by sputtered and rebounding particles. The target (base diameter 6 cm, axial length 9 cm) was constructed of molybdenum plate. To check the values of thrust evaluated using the cone-shaped target, the thrust also was evaluated, using a target made of circular screen with capture ratio of 0.28 (rapture ratio = the area screened by wire mesh/total frontal area).[7] The measured thrust T is used to calculate I_{sp} and η_T.

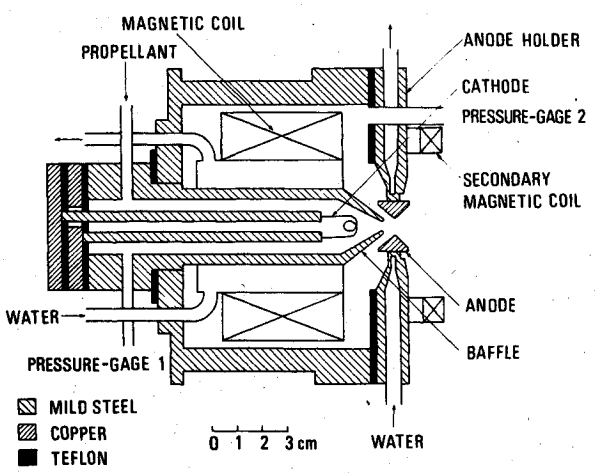

Fig. 1 Schematic of Duoplasmatron-type MPD thruster used.

Received Nov. 12, 1976; presented as Paper 76-1003 at the AIAA International Electric Propulsion Conference, Key Biscayne, Fla., Nov. 14-17, 1976; revision received April 12, 1977.

Index categories: Electric and Advanced Space Propulsion; Plasma Dynamics and MHD.

*Professor, Department of Aeronautics, Faculty of Engineering. Member AIAA.

†Formerly Graduate Student; presently Research Scientist, Institute of Plasma Physics, Nagoya University, Nagoya, Japan.

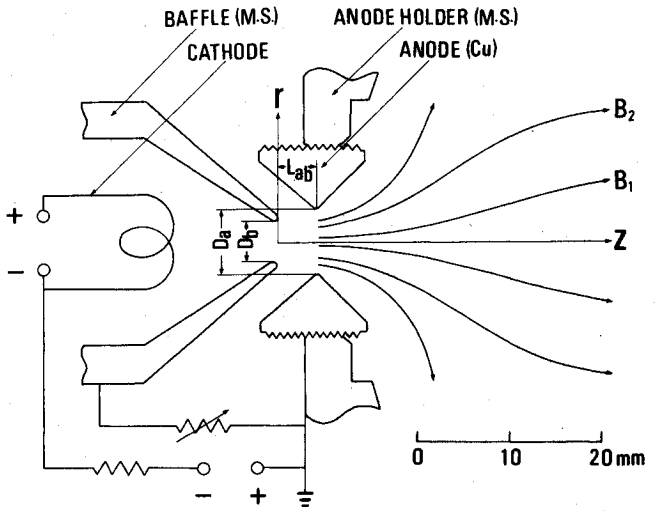

Fig. 2 Detail of electrode geometry and magnetic field map (electrode-geometry A).

$$I_{sp} = T/\dot{m}g \qquad \eta_T = T^2/2\dot{m}P_D$$

The thrust efficiency η_T does not include the power of the magnetic coils and cathode heating.

For thrust measurements, the target method is inferior to the thrust-stand method of other researchers from the standpoint of accuracy, because of some ambiguity in the estimation of momentum accommodation of colliding particles. However, for the case of particles with relatively large mass, such as argon ions, it may be estimated that the momentum accommodation of the particles coming out from the target is tolerable, from the following considerations. The speed of an argon ion is reduced to about 40% of its incident speed by one head-on collision with a molybdenum atom. (It has been pointed out before that, at high collision energies, the collision process of a particle with a surface can be described in terms of an elastic binary collision between the particle and a single "free" surface atom.[8]) If it is assumed that the ion collides twice in the cone-shaped target until it comes out from it, the speed of the ion is reduced to about 16% of its initial value. (In this experiment, in which the exhaust-plume diameter is shorter than the base diameter of the target, the proportion of the particles that come out from the target after only one collision will be very small). It is expected, furthermore, that the mean axial velocity component of the particles coming out from the target is smaller than their speed because of the effect of dispersion. On the other hand, the particles with small mass, such as hydrogen ions, hardly lose their speed by the collision with a molybdenum atom. However, in this case, it is expected that the gas adsorbed at the metal surface contributes to the increase of the momentum accommodation coefficient. (It is well known that adsorbed gas increases the thermal accommodation coefficient.[9]) The background pressure in the present experiments is not sufficiently low to obtain accurate data for thrust. Referring to the experimental results showing the effect of background gas on thrust measurements,[10,11] it may be expected that the error in thrust measurement of the present experiment does not exceed 10%. We suppose that the present experimental results are useful in providing answers to the feasibility question of a plasma thruster of this type, although the background pressure is not sufficiently low, and no correction was made in thrust measurement for the insufficient momentum accommodation of colliding particles.

Plasma Diagnostic Techniques

Electron Temperature and Plasma Potential

A cylindrical electrostatic probe, made of tungsten wire 0.2 mm in diameter and 5 mm in length, was used for the measurements of electron temperature and plasma potential. It is known that the magnetic field applied causes the probe characteristic (current-voltage diagram) to plateau before reaching the true saturation electron current.[12] But, in the present case, the magnetic field is not so strong, and the electron gyro radius is larger than the thickness of electrical sheath formed at the probe surface. So the plasma potential was evaluated by the conventional method, extrapolating electron saturation and transition portions of the diagram. The method of electron temperature evaluation based on transition portion is not affected by the presence of the magnetic field.[12]

Flow Direction and Number Density of Ions

The flow direction of ions was determined by turning the cylindrical electrostatic probe in the flow and observing the direction where ion current is minimum, corresponding to total ion collection by the 0.2-mm diam probe tip. The response of cylindrical probes at various angles of incidence changes with experimental conditions, and it even has been reported that an ion current peak was observed near the zero angle of incidence.[13] However, under the present experimental conditions, where the thickness of electrical sheath (or Debye length λ_D) is small compared with probe diameter d_p and the flow velocity U is very high ($d_p/\lambda_D \gg 1$, $U/\sqrt{kT_e/m_i} \gg 1$), a monotonic increase of the ion current is expected with increasing incidence angle.[14] Once the ion flow direction is determined, the ion number density can be obtained by the standard method,[15] measuring the ion current when the cylindrical probe is parallel to the plasma flow direction.

Flow Velocity of Ions

Flow velocities of ions were determined by comparing the saturation ion current collected by a flat-faced probe (0.5 mm diam) aligned perpendicular to the flow with that collected by a similar probe aligned parallel to it.[16] The uncertainty of the velocity measurement based on this method is relatively large. (In the case of Ref. 16, the estimated uncertainty is reported to be 25%.)

Experimental Results

Performance of Thruster

The best sets of operating data, at a discharge power of nearly 500 W, are shown in Table 1 for five propellants. Figure 3 shows the sets of η_T vs I_{sp} data for the five propellants, obtained by keeping propellant flow rate and magnetic coil current at the values shown in Table 1. An example of the improvement in performance by use of the secondary magnetic coil also is shown for the case of AR propellant (no secondary magnetic coil current: solid line; with secondary magnetic coil current: dotted line). In these experiments, for Ar, N_2, and NH_3 propellants, electrode-geometry A is used, and for He and H_2 propellants, electrode-geometry *B* is used. These experimental results suggest that Ar or NH_3 is substantially superior to other propellants used in this thruster, and that, when Ar or NH_3 is used, thrust efficiencies from 20 to 30% can be obtained in the specific impulse range of 800-3500 sec.

Figure 4 shows a typical example of the effect of variations in the main magnetic coil current on the performance. At zero coil current, the thrust efficiency is very low, but, when the current to the coil is increased up to 3 A, the performance is improved markedly. Over 3 A, performance does not improve appreciably. This experimental result coincides qualitatively with that obtained in a downstream-cathode MPD thruster (a low-power MPD thruster with applied magnetic field).[11]

The optimum value of magnetic coil current increases with increasing propellant flow rate. Figure 5 shows a typical example of the effect of propellant flow rate on the performance. In this case, the magnetic coil current is adjusted to the optimum value for each propellant flow rate. This ex-

Table 1 Typical operating parameters of Duoplasmatron-type MPD thruster

Propellant	Ar	Ar	N_2	NH_3	He	H_2
Propellant flow rate ($\dot{m}$), mg/sec	0.948	0.948	0.339	0.265	0.059	0.021
Main magnetic coil current (I_c), A	6.0	8.0	3.0	3.0	3.0	3.0
Secondary magnetic coil current (I_c'), A	0	5.0	0	0	0	0
Discharge current (J), A	6.0	6.0	4.0	3.0	3.0	3.0
Discharge voltage, V	87	80	146	150	175	175
Discharge power (P_D), W	522	480	584	450	525	525
Thrust (T), mN	16.8	16.7	8.51	7.61	2.04	1.69
T/P_D, mN/kW	32.1	34.8	14.5	16.9	3.9	3.2
Thrust efficiency (η_T), %	28.4	30.6	18.3	24.3	6.7	13.0
Specific impulse (I_{sp}), sec	1810	1800	2560	2930	3530	8210
Power invested in magnetic coils, W	130	236	32	32	32	32
Power invested in cathode heating, W	~100	~100	~100	~100	~100	~100

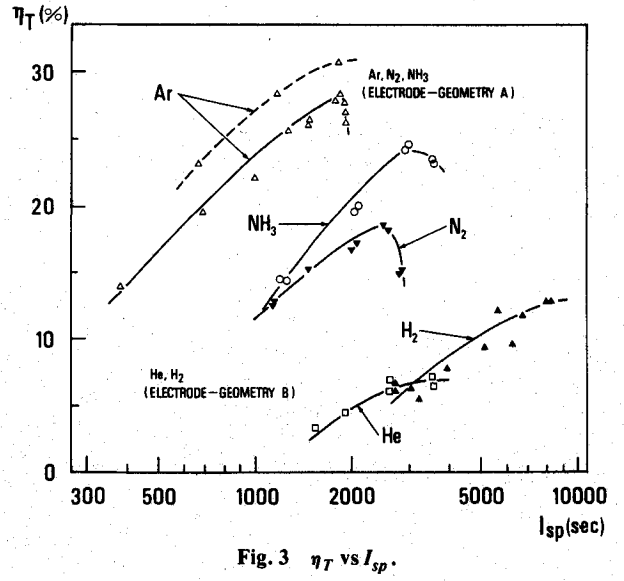

Fig. 3 η_T vs I_{sp}.

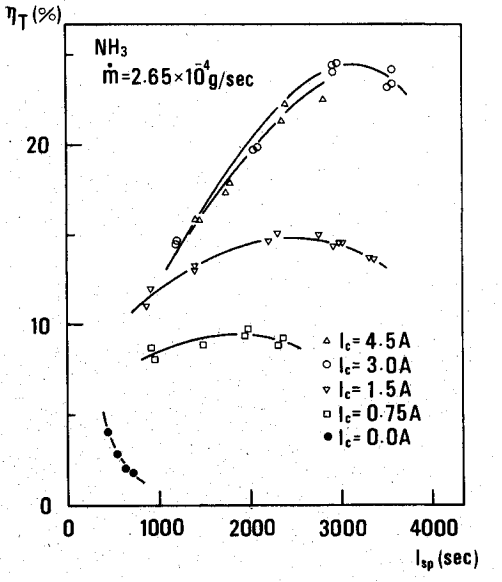

Fig. 4 Effect of magnetic field on performance.

perimental result shows that there exists an optimum flow rate for a given electrode geometry. In Figs. 3-5, it is seen that thrust efficiencies increase with increasing I_{sp}. (This tendency also is shown in Ref. 11). But the values of $J^2/\dot{m}$ at critical conditions, in the present experiment, are far smaller than that in the case of a high-power MPD thruster, in which the acceleration mechanism by self-induced field is prevailing.[17]

Diagnostics of Exhaust Plume

The exhaust plume (argon) formed under the operating condition shown in the first column of Table 1 was selected for diagnostic study. The inside region of the anode throat could not be probed because of extreme heating of the probe. The contours of electron temperature and plasma potential in the plume are shown in Figs. 6 and 7, and their variations along the thruster centerline and the magnetic line of force B_2 (see Fig. 2) are shown in Fig. 8. It is seen in these figures that the potential and the electron temperature decrease in the direction of the flow. A detailed examination of the data of Fig. 8 shows, in addition, that the electron temperature does not decrease as rapidly as one would expect in an adiabatic expansion,[18,19] a tendency that coincides with that obtained in a similar experiment using a small arc plasma thruster.[20]

The result of flow-direction measurements showed an azimuthal ion velocity component, of which direction of rotation coincides with that of E/B drift caused at the anode region. Figure 9 shows the radial profiles of ion number

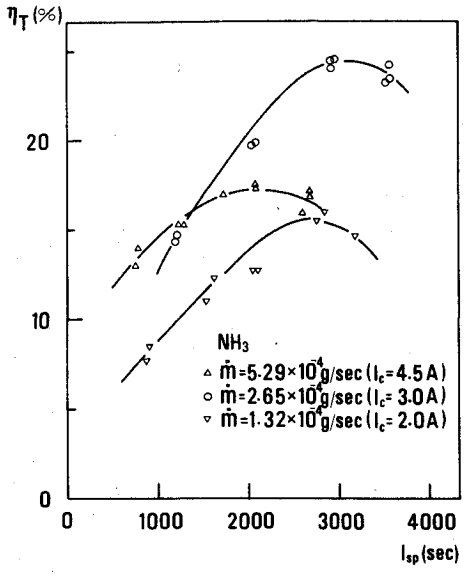

Fig. 5 Effect of propellant flow rate on performance.

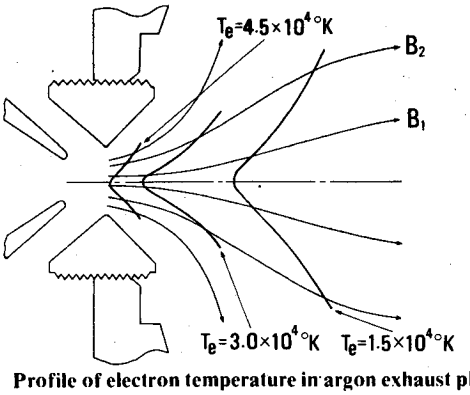

Fig. 6 Profile of electron temperature in argon exhaust plume.

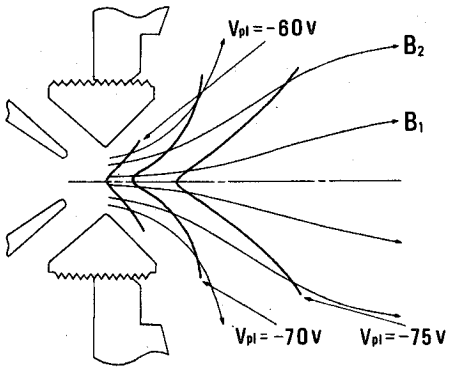

Fig. 7 Profile of plasma potential in argon exhaust plume.

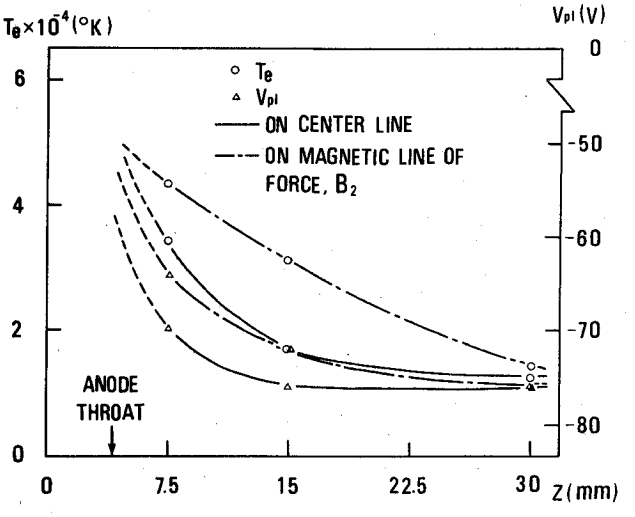

Fig. 8 Variations of electron temperature and plasma potential along thruster centerline and magnetic line of force B_2 (in argon exhaust plume).

density (n_i) and axial component of ion velocity (u_{iz}) obtained at the section $z=30$ mm.

Discussion

Acceleration Mechanisms

The preceding experimental results suggest that the following two electromagnetic acceleration mechanisms exist in this thruster: 1) plasma expansion in a magnetic nozzle, and 2) transformation of rotational energy of ions into kinetic energy of axial direction. For the present experimental conditions, it can be shown that, at the anode area, the orders of electron and ion gyro radii are 1×10^{-2} and 1 mm, respectively (anode throat diameter of 7 mm). Unfortunately, we cannot estimate reliable values of electron and ion Hall parameter at the anode throat area, because of the lack of diagnostic data, and so we have no information on the magnitude of the induced Hall current (azimuthal) at this location. But the Hall current (even if it exists at this throat location) does not produce a force component that yields directed thrust; it produces that which yields containment, since the magnetic field lines are nearly axial at the anode throat area.

Based on the aforementioned two acceleration mechanisms, the values of axial component of ion velocity (u_{iz}) at the section $z=30$ mm were evaluated on the centerline and on the line of force B_2 ($r=13$ mm), using the results of Fig. 8. In this case, it is assumed that, at the throat of the anode nozzle, the axial component of ion velocity is equal to the speed of sound $\sqrt{kT_e/m_i}$ and the azimuthal component of velocity E/B. On the centerline, an ion is accelerated corresponding to the potential drop, and its velocity (axial) can be calculated using the energy equation:

$$\tfrac{1}{2}m_i(u_{i\infty}^2-u_{i0}^2)=e(V_{pl0}-V_{pl\infty})$$

where m_i is ion mass, e electronic charge, u_i ion speed, V_{pl} plasma potential, and subscript 0 indicates the position of the anode throat, and subscript ∞ indicates a position in the downstream region (in this case $z=30$ mm). For the evaluation of the axial component of ion velocity on the line of force B_2, the contribution of rotational motion induced at the anode throat area is taken into consideration further, using the relation of conservation of angular momentum. (In this case, it is assumed that an ion moves downwards, confined to the surface formed by rotating the line of force B_2.) The obtained value of u_{iz} on the centerline was 9.4×10^3 m/sec, and that on the line of force B_2 was 2.4×10^4 m/sec. These values are in reasonable agreement with the experimental values in Fig. 9, which suggests that the aforementioned two acceleration mechanisms can be the prevailing ones in the thruster of this type.

Calculation of Ionization Efficiency and Thrust

The calculation of total ion flux at the section of $z=30$ mm, using the results shown in Fig. 9, yields a value of 1.37×10^{19} sec^{-1}, which corresponds to a propellant ionization efficiency of 97%. Although the accuracy of the data of n_i and u_{iz} shown in the figure is not sufficient for detailed quantitative discussions, this matter indicates that, in this thruster, the ionization efficiency is fairly high under the proper

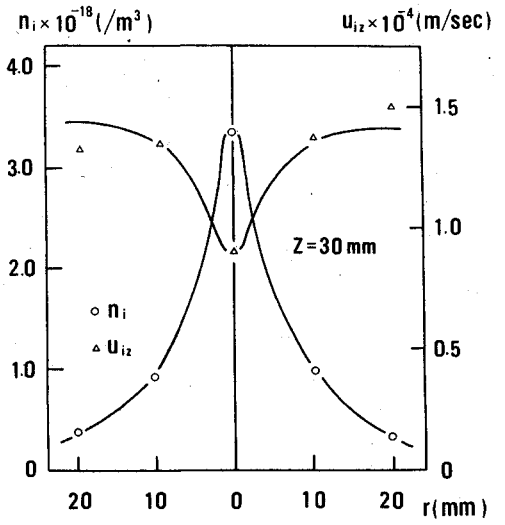

Fig. 9 Radial profiles of ion number density and axial component of ion velocity at the section of $z = 30$ mm (in argon exhaust plume).

operating conditions. The calculation of total momentum flux (ion) at the same section yields a value of 13.8 mN, which is 18% less than the value of thrust measured by the target method (16.8 mN). The discrepancy may be attributed to some error in the measurement of ion flow velocity or thrust, or to the possibility that, at $z = 30$ mm, the acceleration of plasma in the axial direction is not brought to completion yet.

Concluding Remarks

Substantial improvement in the thrust performance of a Duoplasmatron-type low-power MPD thruster has been achieved. When Ar or NH_3 propellant is used, thrust efficiencies from 20 to 30% can be obtained in the specific impulse range of 800-3500 sec. For the practical use of a thruster of this type, however, the problems of cathode life and baffle-tip cooling by suitable methods still must be solved. Detailed examinations of the data, obtained by diagnostic measurements, show that the ionization efficiency of propellant is fairly high and that, in this thruster, the following two prevailing mechanisms exist for the plasma acceleration: 1) plasma expansion in a magnetic nozzle, and 2) transformation of rotational energy of ions into kinetic energy of axial direction.

References

[1] Burkhart, J.A., "Performance of a Modified Downstream-Cathode MPD Thruster," *Journal of Spacecraft and Rockets,* Vol. 10, Jan. 1973, pp. 86-88.

[2] Vondra, R.J. and Thomassen, K.I., "Flight Qualified Pulsed Electric Thruster for Satellite Control," *Journal of Spacecraft and Rockets,* Vol. 11, Sept. 1974, pp. 613-617.

[3] Palumbo, D.J. and Guman, W.J., "Effect of Propellant and Electrode Geometry on Pulsed Ablative Plasma Thruster Performance," *Journal of Spacecraft and Rockets,* Vol. 13, March 1976, pp. 163-167.

[4] Kimura, I. and Kumazawa, R., "A Low-Power MPD Thruster of Duoplasmatron Type," *Journal of Spacecraft and Rockets,* Vol. 10, July 1973, pp. 472-473.

[5] von Ardenne, M., *Tabellen der Elektronenphysic, Ionenphysik und Ubermikroskopie,* VEB Deutscher Verlag der Wissenschaften, Berlin, 1956, p. 55.

[6] Kerslake, W.R. and Pawlik, E.V., "Additional Studies of Screen and Accelerator Grids for Electron-Bombardment Ion Thrusters," NASA TN D-1411, 1963.

[7] Fradkin, D.B., Blackstock, A.W., Roehling, D.J., Stratton, T.F., William, M., and Liewer, K.W., "Experiments Using a 25-kw Hollow Cathode Lithium Vapor MPD Arcjet," *AIAA Journal,* Vol. 8, May 1970, pp. 886-894.

[8] Smith, D.P., "Analysis of Surface Composition with Low-Energy Backscattered Ions," *Surface Science,* Vol. 25, March 1971, pp. 171-191.

[9] Eckert, E.R.G. and Drake, R.M., *Analysis of Heat and Mass Transfer,* McGraw-Hill, New York, 1972, pp. 479-484.

[10] Sovie, R.J., and Connolly, D.J., "Effect of Background Pressure on Magnetoplasmadynamic Thruster Operation," *Journal of Spacecraft and Rockets,* Vol. 7, March 1973, pp. 255-258.

[11] Burkhart, J.A. "Exploratory Tests on a Downstream-Cathode MPD Thruster," *Journal of Spacecraft and Rockets,* Vol. 8, March 1971, pp. 240-244.

[12] Chen, F.F., *Plasma Diagnostic Techniques,* Academic Press, New York, 1965, pp. 162-177.

[13] Sonin, A.A., "Free-Molecule Langmuir Probe and Its Use in Flowfield Studies," *AIAA Journal,* Vol. 4, Sept. 1966, pp. 1588-1596.

[14] Iachetta, F.A. and Smetana, F.O., "Experiments on the Current Collected by a Cylindrical Langmuir Probe in a Rarefied Plasma Streaming with High Velocity," *Rarefied Gas Dynamics,* Vol. II, Academic Press, New York, 1969, pp. 1783-1790.

[15] Laframboise, J.G., "Theory of Spherical and Cylindrical Langmuir Probes in a Collisionless, Maxwellian Plasma at Rest," Univ. of Toronto, Inst. of Aerospace Studies, Rept. 100, June 1966.

[16] Chubb, D.L., "Double Electrostatic Probe for Measuring Density, Temperature, and Velocity of a Flowing Plasma," NASA TN D-7223, 1973.

[17] Malliaris, A.C., John, R.R., Garrison, R.L., and Libby, D.R., "Performance of Quasi-Steady MPD Thrusters at High Power," *AIAA Journal,* Vol. 10, Feb. 1972, pp. 121-122.

[18] Walker, E.L. and Seikel, G.R., "Axisymmetric Expansion of a Plasma in a Magnetic Nozzle Including Thermal Conduction," NASA TN D-6154, 1971.

[19] Kosmahl, H.G., "Three-Dimensional Plasma Acceleration through Axisymmetric Diversing Magnetic Fields Based on Dipole Moment Approximation," NASA TN D-3782, 1967.

[20] Bowditch, D.N., "Investigation of the Discharge and Exhaust Beam of a Small Arc Plasma Thruster," AIAA Paper 66-195, 1966.